Molecular Dynamics Study of Uncharged Bupivacaine Enantiomers in Phospholipid Bilayers

M. Florencia Martini[a,b] and Mónica Pickholz*[a,b]

To investigate the effects of the uncharged bupivacaine (BVC) on the properties of model membranes of 1-palmitoyl-2-oleoyl-sn-glycero-3-phosphatidylcholine (POPC), we have performed a series of molecular dynamics simulations. A very particular characteristic of the local anesthetic BVC, that is being discuss in the recent literature, is that their enantiomers R-(+) (R-BVC) and S-(−) (S-BVC) present different activities. In this way, we have studied both enantiomers in a POPC phospholipids bilayers at a high molar ratios [local anesthetic (LA):lipid of 1:3]. The simulations were able to capture important features of the BVC–phospholipid bilayer interactions: BVC molecules are found in the interior of the bilayer. The R-BVC enantiomer follows a bimodal distribution with access to the water–lipid interface; while the S-BVC is found, in more uniform distribution, at the hydrophobic region. A decrease in the acyl chain segment order parameters, S_{CD}, compared to neat bilayers, is found. Furthermore, this behavior is more noticeable for the R-BVC form. The found decrease in S_{CD} is attributed to a larger accessible volume per lipid in the tail region. Our results could help to understand the higher toxicity of this enantiomer. © 2012 Wiley Periodicals, Inc.

DOI: 10.1002/qua.24208

Introduction

Local anesthetics (LAs) are pain relief drugs. Bupivacaine (BVC) is an amino-amide local anesthetic with pKa of 8.1. In this way, BVC are partitioned in neutral and protonated forms at physiological pH. The anesthetic action of BVC, as most of LA, is based on its ability to block the voltage gated Na^+ channels in the nervous system. The BVC (in a racemic mixture) is one of the most widely used LA, due to its quality of anesthesia and prolonged duration of action; however, it presents high toxicity. A very particular characteristic of BVC is that their enantiomers, R-(+) and S-(−), present different activities. Both enantiomers are active as nerve blockers. However, the R-(+) is more toxic than the S-(−) form. It was suggested in the literature that BVCs stereoisomers would interact differently with biomembranes at cardiotoxically relevant concentrations.[1,2] In this way, a good understanding of the interaction of each enantiomer with biological membranes could provide insights to improve their efficacy and minimize their side effects. The advantage of the neutral species is related to their stronger binding to the membrane. In fact, their dispersion into the bilayer could provide a way to protect the molecule from metabolism process that could produce their elimination.[3] As a result, it is expected a clearance delay, justifying long-lasting anesthesia. Indeed, good evidence for this hypothesis is given by the observation that hydrophobic anesthetics show longer half-lives than hydrophilic ones.[4]

In this work, we study the interaction of the S- (S-BVC) and R- (R-BVC) forms of BVC, at their uncharged (neutral) ionization state, in model lipid membranes, at high lipid drug molar concentrations through molecular dynamics (MD) simulations. The MD technique has been shown as a very powerful tool for studying the interaction of LAs with membranes.[5–8]

In next section, we described the methodology and simulation setup used in this work, followed from a brief discussion of the structure of neutral BVC enantiomers. In the results section, we show different analysis that have been done from the simulation run trajectories, comparing the effects of the enantiomers R- and S-. The last section is devoted to the final discussion.

Simulation Setup

The simulated systems consist of a lipid bilayer containing 120 1-palmitoyl-2-oleoyl-sn-glycero-3-phosphatidylcholine (POPC) lipids (60 in each monolayer) fully hydrated and 40 neutral S-BVC and R-BVC, respectively (lipid:drug molar ratio 3:1). This concentration was chosen following experimental conditions in model membranes.[9] We take into account periodic boundary conditions. The initial structures were built using packmol package.[10] Both BVCs species were originally placed in the interior of the bilayer.

Classical MD simulations were performed within the *NPT* ensemble (*P* = 1 atm and *T* = 310 K). The size of the simulation cell was fully flexible (keeping the constraint in *XY* dimensions, *Lx* = *Ly*). Langevin dynamics and Langevin piston methods were used to keep temperature and pressure constant.

[a,b] M. F. Martini, M. Pickholz
Department of Pharmaceutical Technology, Faculty of Biochemistry and Pharmacy, University of Buenos Aires, Junín 956, Buenos Aires, Argentina
CONICET, Buenos Aires, Argentina
E-mail: mpickholz@gmail.com

© 2012 Wiley Periodicals, Inc.

Following standard procedures, the simulation of each system consisted of an equilibration period of about 20 ns, within which the guest molecules migrated to their preferential location relative to the membrane, followed by at least 50 ns of a production run. A multiple-time step algorithm, RESPA,[11] was used with the shortest time step of 2 fs. The short-range forces were computed using a cutoff of 10 Å and the long-range forces were taken into account by means of the particle mesh Ewald technique.[12]

Simulations were performed using the NAMD2 program[13] with the PARAM27 CHARMM parameter set[14] and the water molecules were described by the TIP3P model.[15] No parameters are available in the literature for this molecule and, therefore, we based our parameterization, including intramolecular bond lengths, angles and dihedrals on the equilibrium geometry, as we described below, consistently with the parameterization of similar anesthetics.[7,16] The force constants and intermolecular parameters were chosen in analogy to similar molecules already described by CHARMM parameter set.[14] The topology and the full set of parameters used for the BVCs are included as Supporting Information Material.

Structure of Neutral BVCs

The ground state geometry of both the enantiomers of neutral BVC was optimized within the density functional theory using the B3LYP[17] functional and 6-311G** basis set. The molecular structures of the enantiomers R-BVC and S-BVC are shown in Figure 1. The main conformational differences between the enantiomers that we would like to remark here is the relative orientation between the aromatic and saturated rings: in R-BVC they are perpendicular, while for S-BVC, they are almost coplanar. For instance, the dihedral between the two nitrogens (NCCN) is an example of this: 138° and 89° for the S-BVC and R-BVC, respectively.
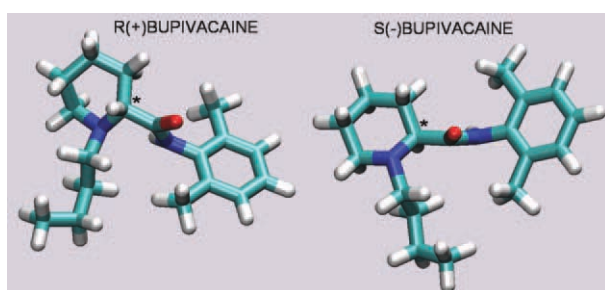

Figure 1. Molecular structure of R-BVC and S-BVC. [Color figure can be viewed in the online issue, which is available at wileyonlinelibrary.com.]

The partial atomic charges were obtained from a single-point HF/6-31G* calculation using Gaussian[18] and the Merz–Singh–Kollman protocol.[19] We would like to mention here that no remarkable differences were found between the charge distribution of the S-BVC and R-BVC species (see Supporting Information Material). The dipole moments did not differ considerably between both species (3.76 Debye and 3.53 Debye, respectively).

Simulation Results

Here, we show the main analysis done over the 50 ns of the production run of the S-BVC and R-BVC in POPC lipid bilayers. For comparison purpose, in some cases, we also discuss the results of a neat POPC lipid bilayer.

Simulation box

The area per lipid, A_{lip}, is defined as the length of the simulation box in the X-dimension multiplied by the box length in the Y-dimension divided by the number of lipids per monolayer. In Table 1, we show the average A_{lip}, S-BVC, and R-BVC containing POPC bilayers. For comparison effects, we have also included the results of a neat POPC lipid bilayer in the table. We can see from this table a remarkable increase of the area per lipids when the BVCs are present respect to the neat bilayer. In particular, the A_{lip} is ~8 Å^2 greater for the R-BVC than for the S-BVC case. Furthermore, the z-dimension of the simulation box, z_{box}, also included in Table 1, shows opposite behavior: it is ~7 Å shorter for the R-BVC than for the S-BVC. These results suggest difference behavior of the S-BVC and R-BVC species in lipid membranes. Besides, the box volume is slight bigger, ~300 Å^3 (0.1%), for the R-BVC case than for the S-BVC showing a worse packing of the R-BVC molecules within the bilayer. To see further differences and understand the behavior of the two enantiomers, we look at the membrane organization and drug effects in more detail in the following subsections.

Table 1. Area per lipid (A_{lip}), Z-dimension of the simulation box (Z_{box}), and distance between phosphate for the neat bilayer and the two bilayers containing BVC.

	Neat bilayer	S-BVC/POPC	R-BVC/POPC
A_{lip} (Å^2)	58.14(1)	68.57(1)	76.29(1)
Z_{box} (Å)	71.72(1)	67.42(1)	60.75(1)
P—P dist. (Å)	36.3(2)	38.2(2)	29.7(5)

Electron density profiles

The electron density profiles (EDPs) were calculated by time averaging the net charges per 0.1 Å thick slabs. We have calculated the EDP of the whole bilayer as well as it different components. The $z = 0$ corresponds to the bilayer center.

In Figure 2, we show the EDPs as function of the z direction of both bilayer under study: S-BVC-bilayer (solid lines) and R-BVC-bilayer (dash lines). The different groups are plotted separately: POPC is displayed in black, water in blue, and S-BVC and R-BVC in red and green, respectively. Comparing POPC EDPs, we can see different features between both bilayers: the S-BVC bilayer present a similar characteristic to the plain bilayer, where a lower density is observed at the bilayer center, while the R-BVC-bilayer shows a more uniform distribution at the hydrophobic region. The bilayer thickness could be estimated from the distance between maxima of the POPC distribution (essentially corresponds to the phosphorous–phosphorous distance) and it is displayed in Table 1. In this way, the bilayer thickness is remarkably shorter for the R-BVC-bilayer
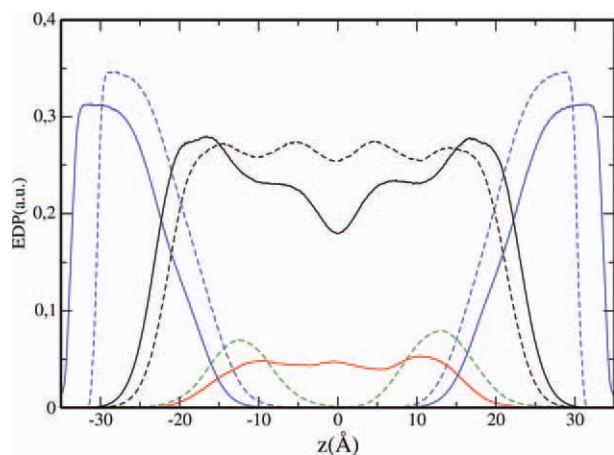
Figure 2. EDP as function of the z-axis. Solid and dashed lines correspond to the S-BVC and R-BVC bilayers, respectively. Colors used for the different bilayers components: POPC in black, water in blue, S-BVC in red, and R-BVC in green. [Color figure can be viewed in the online issue, which is available at wileyonlinelibrary.com.]

with respect to the S-BVC-bilayer ($\sim$8.5 Å), pointing out major organization difference between enantiomers. The EDP for water (blue lines) drops from the bulk aqueous phase value to zero, as an essentially dry lipid tail region is reached passing through an intermediate complex lipid–water interfacial region in which the polar headgroups are hydrated, which shows the bilayer organization of the system. The distribution of the neutral R-BVC shows a bimodal distribution with little access to the lipid water interface, similar to the one found for general anesthetics,[20] lidocaine,[6] and prilocaine.[21] The maxima are essentially at a distance of $\sim$12Å from the center of the bilayer, in the hydrophobic region of the membrane with almost zero density at the membrane center. Even if this value is similar with the found for other anesthetics, such as prilocaine,[7] due to the different organization of both bilayers, it lies in a more hydrophilic region. By the other hand, the distribution of S-BVC is remarkable different: it has a more uniform distribution with little access to the water lipid interface, showing the characteristics of a more hydrophobic LA.[22]

Furthermore, details about the LAs orientation can be obtained by analyzing the distribution of the main groups of the BVC's molecules. In this case, we have studied separately the aromatic and saturated rings for both cases. These results are not shown here. However, we would like to remark that in average neither R-BVC nor S-BVC show specific orientation within the bilayer. Furthermore, we do not find specific interactions between the BVC molecules with the POPC lipids of the bilayers. On the other hand, as was already discussed, there are structural differences between both species that could affect their distribution within the membrane. In particular, we look at the relative orientation between the aromatic and saturated ring. In this direction, we have defined the V_1 and V_2 vectors, shown in onset of Figure 3, as the difference of two carbon atoms of each of the rings. The angle between them, $\theta = \arccos(V_1 \cdot V_2 / |V_1 \| V_2|)$, provides an idea of their relative orientation. In Figure 3, we show the histograms of θ angle occurrence, averaged in time and molecule number for R-BVC (green) and
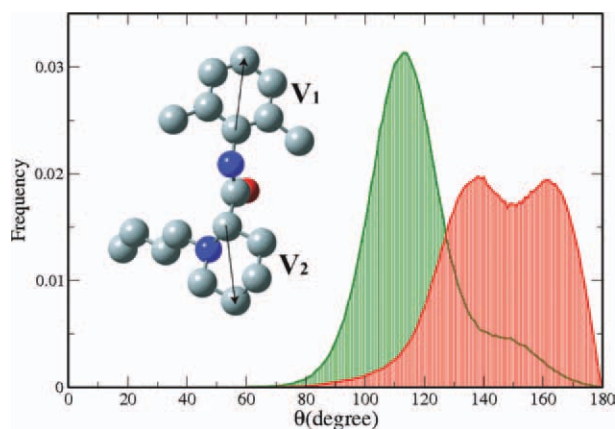

Figure 3. Histogram of the θ angle frequency for R-BVC (green) and S-BVC (red) molecules. The angle θ is the one formed by the V_1 and V_2 vectors, as shown in the onset scheme of this figure. [Color figure can be viewed in the online issue, which is available at wileyonlinelibrary.com.]

S-BVC (red). We can see from this figure a remarkable different conformation: R-BVC shows a more defined peak around $\sim$120° (in a more compact geometry), whereas S-BVC has a broader distribution in the range of 125–180°. In this way, the more co-planar conformation of S-BVC makes it smoother to diffuse into the bilayer.

BVCs center of mass trajectories

As we show, the S-BVC EDP shows a dense distribution in the center of the membrane, this suggest that S-BVC can cross between the two monolayers. In Figure 4, we show the center-of-mass trajectory along interface normal (z) evolution in time for five (representative) molecules of the 40 S-BVC. We can see from this figure that some of the molecules cross from one monolayer to the other (red and black), others remain always in the some monolayer (blue and violet). We consider crossing event when the molecule cross from one monolayer to the other reaching at least $\pm$5Å of the other monolayer, for at least 0.2 ns. In this way, we observe molecules with crossing events in the range of 0–3. In particular,
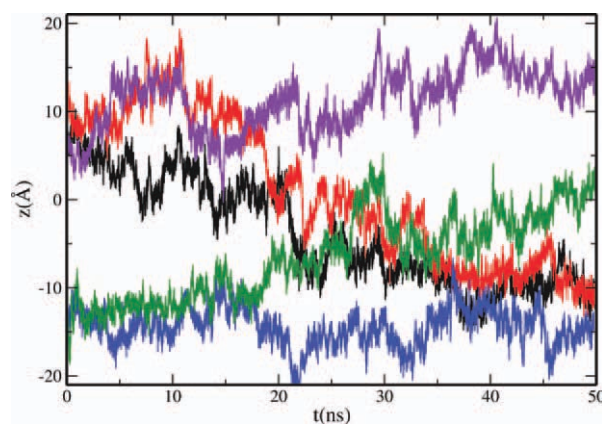

Figure 4. Trajectories of the center of mass z-coordinate of five S-BVC molecules in the bilayer. [Color figure can be viewed in the online issue, which is available at wileyonlinelibrary.com.]

the green trajectory (Fig. 4) is computed as 0, as the molecule starts in the lower monolayer and cross to the other; however, it remains oscillating in the middle of the bilayer. In this way, during the 50 ns, we identified 29 crossing events.[6] It can be readily seen that the 50 ns runs were sufficiently long time to see S-BVC hopping from one monolayer to the other.

On the other hand, in Figure 5, we show the CM trajectories of every R-BVC over 50 ns. We did not observe any crossing events during the simulation run. We can see in this figure that few of them reach the middle of the bilayer, however, they got back to the starting monolayer.
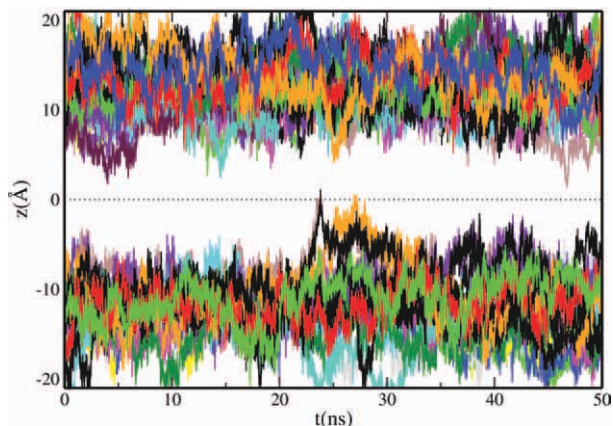

Figure 5. Trajectories of the center of mass z-coordinate of each of the R-BVC molecules in the bilayer. [Color figure can be viewed in the online issue, which is available at wileyonlinelibrary.com.]

Order parameters

One of the most popular quantities to characterize order in lipid bilayers is the order parameter defined by:

$$S_{mol} = \frac{1}{2}\langle 3\cos^2\theta_n - 1 \rangle,$$

where θ_n is the angle between the normal to the bilayer and the normal to the plane defined by in $C(n)H_2$ of the n carbon of the methylene group of the lipid acyl chain. The order parameter is related to the tilt angle of the chains and to trans-gauche distribution of chain dihedrals, but the relationship is indirect. The experimental order parameter, $S_{CD} = -1/2\, S_{mol}$, is derived from the measured residual quadrupole splitting $\Delta v = (3/4)(e^2qQ/h)S_{CD}$.[23]

The order parameters of each C—H methylene groups have been calculated for every case. The CH_2 groups are numbered consecutively.[7] In Figure 6, we show the order parameter as of each carbon of POPC tail. We separate the (a) palmitoyl and (b) oleoyl tails. As a reference, we show in black the order parameter for plain POPC in good agreement with the results found by other authors.[24] The overall effect of R-BVCs (at 1:3 molar concentration) is to disorganize the membrane (decrease the order parameters); this effect is seen for both tails. However, it is more pronounced from carbons higher than 6 and 10, for the palmitoyl and oleoyl lipid tails, respectively. This is essentially related with the empty space in the lower part of the lipid tails due to the localization of the LA and the lateral expansion of
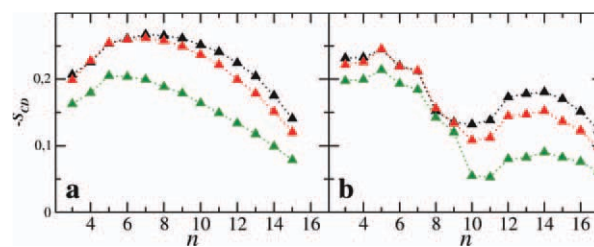

Figure 6. The order parameter, $-S_{CD}$, for plain bilayers (black) and S-BVC and R-BVC containing bilayer in red and green, respectively, along with the order parameter along the hydrocarbon chain for a) saturated and b) unsaturated tails of POPC. [Color figure can be viewed in the online issue, which is available at wileyonlinelibrary.com.]

the bilayer. On the other hand, S-BVC only promotes a soft disorganization for carbons above 10 (in both tails): in this case, the localization of the LA in the interior of the bilayer compensate the effects of the lateral expansion.

PN vector

The effects of BVCs on the lipid headgroups of the bilayers can be analyzed in more detail by inspecting the orientation probability distribution of the charged groups P and N of the zwitterionic lipid heads. Let θ be the angle between the $P^-_3N^+$ vector and the monolayer normal.

An angle of $0°$ corresponds to a vector aligned with the axis of reference pointing toward the aqueous phase, and an angle of $180°$ corresponds to a vector pointing toward the monolayer hydrocarbon tails.[25] The orientation probability distributions, $P(\theta)/P^{ISO}(\theta)$, calculated by averaging over all lipids and all configurations are depicted in Figure 7 for the control neat bilayer (black) and S-BVC and R-BVC bilayers in red and green, respectively. In the control, the preferential orientation is around $\theta \sim 80°$. The orientation of the POPC lipid heads seems not to be affected by the presence of S-BVC bilayers. On the other hand, the presence of R-BVC changed the orientation going to $\sim 70°$. Taken into account that no preferential orientation was found for these molecules inside the bilayers, this change could contribute to change the membrane polarization.
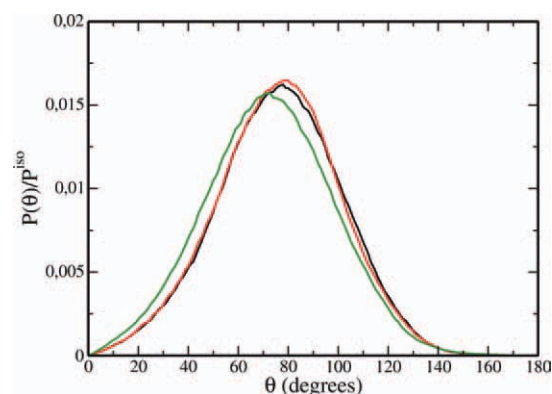

Figure 7. Orientational distribution, $P(\theta)/P^{ISO}(\theta)$, of the θ angle between the headgroup PN vector and the bilayer normal for POPC bilayers. Neat (black), and S-BVC and R-BVC containing bilayer in red and green, respectively. [Color figure can be viewed in the online issue, which is available at wileyonlinelibrary.com.]

Discussion

The role of unprotonated (neutral) LAs has been widely discussed in the literature to understand the mechanism of anesthesia. In this article, we investigate the effects of the two enantiomers, S and R, of neutral BVC in phospholipid bilayer. For that purpose, we performed more than 70 ns MD simulations of a POPC lipid bilayer containing neutral BVC at high drug:lipid ratio (1:3).

From our results, we can say that most of the differences are related with the different spatial structures of the R-BVC and S-BVC forms: S-BVC and R-BVC have different effects over the lipid bilayers. S-BVC, localized essentially in the hydrophobic region of the lipid bilayer, shows a high rate of crossing events between monolayers when we look to the center of mass trajectories. On the other hand, R-BVCs show a bimodal distribution in the upper part of lipid tail with access to the lipid–water interface, showing a concomitant lateral expansion, with respect to the S form. Besides, the effect on the disorganization of the bilayer is more accentuated in presence of the R form. Furthermore, we have not seen any crossing event for the R-BVC case, during the simulation time. It is well known that an increase of membrane fluidity is related to the blockade of cardiac sodium currents.[26–28] Drugs that increase membrane fluidizing also influence the permeability of membranes and the activity of cardiac receptors embedded in plasma membranes.[29,30] In this way, the considerable change in the area per lipid molecule and the disorganization of the lipid tails that the R enantiomer causes in the lipid membrane, showed by our results, could be related with the higher cardiotoxicity effect that generates this form of BVC.

Acknowledgments

[1] H. Tsuchiya, M. Mizogami, *Anesth. Analg.* **2012**, *114,* 310.
[2] H. Tsuchiya, T. Ueno, K. Takamura, *Chem. Biol. Interact.* **2010**, *183,* 19.
[3] L. F. Fraceto, L. M. A. Pinto, L. Franzoni, A. A. C. Braga, A. Sisni, S. Schreier, E. de Paula, *Biophys. Chem.* **2002**, *99,* 229.
[4] (a) B. G. Covino, H. G. Vassalo, Local Anesthetics: Mechanism of Action and Clinical Use; Grune and Stratton: New York, **1976**; (b) T. Narahashi, M. Yamada, *J. Pharmacol. Exp. Ther.* **1970**, *171,* 32.
[5] M. Pasenkiewicz-Gierula, T. Róg, J. Grochowski, P. Serda, R. Czarnecki, T. Librowski, S. Lochynski, *Biophys. J.* **2003**, *85,* 1248.
[6] C.-J. Högberg, A. Maliniak, A. P. Lyubarstsev, *Biophys. J.* **2007**, *125,* 416.
[7] M. Pickholz, L. F.Fraceto, E. de Paula, *Int. J. Quantum Chem.* **2008**, *108,* 2386.
[8] M. Pickholz, G. Giupponi, *J. Phys. Chem. B* **2010**, *114,* 7009.
[9] E. de Paula, S. Schreier, *Biochim. Biophys. Acta* **1995**, *1240,* 25.
[10] J. M. Martínez, L. Martínez., *J. Comput. Chem.* **2003**, *24,* 819.
[11] M. E. Tuckerman, B. J. Berne, G. J. J. Martyna, *Chem. Phys.* **1992**, *97,* 1990.
[12] T. Darden, D. York, L. J. Pedersen, *J. Chem. Phys.* **1993**, *98,* 10089.
[13] L. Kalé, R. Skeel, M. Bhandarkar, R. Brunner, A. Gursoy, N. Krawetz, J. Phillips, A. Shinozaki, K. Varadarajan, K Schulten, *J. Comput. Phys.* **1999**, *151,* 283.
[14] B. R. Brooks, R. E. Bruccoleri, B. D. Olafson, D. J. States, S. Swaminathan, M. Karplus, *J. Comput. Chem.* **1983**, *4,* 187.
[15] W. L. Jorgensen, J. Chandrasekhar, J. D. Madura, *J. Chem. Phys.* **1983**, *79,* 926.
[16] M. Pickholz, L. F. Fraceto, E. de Paula, *Synth Met.* **2009**, *159,* 217.
[17] A. D. Becke, *J. Chem. Phys.* **1993**, *98,* 5648.
[18] M. J. Frisch, G. W. Trucks, H. B. Schlegel, G. E. Scuseria, M. A. Robb, J. R. Cheeseman, V. G. Zakrzewski, J. J. A Montgomery, R. E. Stratmann, J. C. Burant, S. Dapprich, J. M. Millam, A. D. Daniels, K. N. Kudin, M. C. Strain, O. Farkas, J. Tomasi, V. Barone, M. Cossi, R. Cammi, B. Mennucci, C. Pomelli, C. Adamo, S. Clifford, J. Ochterski, G. A. Petersson, P. Y. Ayala, Q. Cui, K. Morokuma, D. K. Malick, D. Rabuck, K. Raghavachari, J. B. Foresman, J. Cioslowski, J. V. Ortiz, B. B. Stefanov, G. Liu, A. Liashenko, P. Piskorz, I. Komaromi, R. Gomperts, R. L. Martin, D. J. Fox, T. Keith, M. A. Al-Laham, C. Y. Peng, A. Nanayakkara, C. Gonzalez, M. Challacombe, P. M. W. Gill, B. Johnson, W. Chen, M. W. Wong, J. L. Andres, C. Gonzalez, M. Head-Gordon, E. S. Replogle, J. A. Pople, GAUSSIAN98 (Revision A.7); Gaussian Inc.: Pittsburgh, PA, **1998**.
[19] (a) U. C. Singh, P. A. Kollman, *J. Comput. Chem.* **1984**, *5,* 129; (b) P. Cieplak, P. A. Kollman, *J. Comput. Chem.* **1991**, *12,* 1232.
[20] M. Pickholz, L. Saiz, M. L. Klein, *Biophys. J.* **2005**, *88,* 1524.
[21] L. F. Cabeça, M. Pickholz, E. de Paula, A. J. Marsaioli, *J. Phys. Chem. B* **2009**, *113,* 2365.
[22] M. Pickholz, L. F. Fraceto, E. de Paula, *Synth Met.* **2009**, *159,* 2157.
[23] (a) J. Seelig, *Quart. Rev. Biophys.* **1977**, *10,* 353; (b) L. J. Burnett, B. H. J. Muller, *J. Chem. Phys.* **1971**, *55,* 5829.
[24] F. Suits, M. C. Pitman, S. E. Feller, *J. Chem. Phys.* **2005**, *122,* 244714.
[25] S. Leekumjorn, A. K. Sum, *Biophys. J.* **2006**, *90,* 3951.
[26] R. A. Harris, P. Bruno, *J. Neurochem.* **1985**, *44,* 1274.
[27] W. R. Leifert, E. J. McMurchie, D. A. Saint, *J. Physiol.* **1999**, *520,* 671.
[28] M. S. Awayda, W. Shao, F. Guo, M. Zeidel, W. G. Hill, *J. Gen. Physiol.* **2004**, *123,* 709.
[29] J. Wang, G. J. Zhang, *Cell Biol. Int.* **2005**, *29,* 393.
[30] Z. Ma, J. B. Meddings, S. S. Lee, *Am. J. Physiol.* **1994**, *267,* G87.